Ethylene and Propylene Polymerization over Chiral *ansa*-Dichloro[*o*-phenylenedimethylenebis(η^5-1-indenyl)]zirconium [$Zr\{C_6H_4(CH_2\text{-}1\text{-}C_9H_6)_2\text{-}1,2\}Cl_2$]

Taek Kyu Han,[†] Byung Won Woo,[‡] Joon T. Park,*[,‡] Youngkyu Do,[‡] Young Soo Ko,[†] and Seong Ihl Woo*[,†]

Departments of Chemical Engineering and of Chemistry, Korea Advanced Institute of Science and Technology, Taejon 305-701, Korea

Received September 28, 1994; Revised Manuscript Received February 23, 1995[®]

ABSTRACT: *ansa*-Dichloro[*o*-phenylenedimethylenebis(η^5-1-indenyl)]zirconium (**1**) has been prepared from the reaction of dilithiated bis(1-indenyl)-*o*-xylene with $ZrCl_4$ in tetrahydrofuran. A *rac*-**1**/*meso*-**1** ratio close to 1 is obtained, and the diastereomeric complexes have been separated by fractional crystallization. Polymerizations of both ethylene and propylene with *rac*-**1** and *meso*-**1** in the presence of methylaluminoxane (MAO) as cocatalyst have been examined. In ethylene polymerization, *meso*-**1** is more active than *rac*-**1**, while in propylene polymerization, the latter is much more active than the former. The polymerization data and the stereochemical analysis of the obtained polypropylene (PP) by ^{13}C NMR spectroscopy reveal that both the activity of the *rac*-**1**/MAO catalyst and the stereoregularity of PP are low due to the distortion of catalyst *rac*-**1** from the C_2 symmetry and the fluxionality of the *ansa*-ligand, which is caused by the four carbon atoms of the rigid *o*-phenylenedimethylene bridge.

Introduction

The α-olefin polymerization is influenced by changes in the structure of *ansa* chiral metallocene catalysts such as variation of the transition metal, the steric and electronic properties of π- and σ-ligands, and the length and rigidity of the bridging groups.[1–8] The activity and the stereoselectivity of olefin polymerization reactions can be significantly affected by slight structural variations of the bridging group in metallocene catalysts. The length of the bridging chain affects the angle between the Cp centeroids and the metal atom. The chiral metallocenes having π-ligands bridged with one atom (carbon or silicon)[9–12] or two carbons[13–15] have either C_2 (*racemic*) or C_s (*meso*) symmetry if the *ansa*-ligand is enantiotopic. The long and rigid bridging group may destroy the symmetry and exert an influence on the overlapping of Cp rings in both the *rac*- and *meso*-forms. Brintzinger and co-workers[16] reported the first *ansa*-titanocene derivative, $^nPr(IndH_4)_2TiCl_2$ (**3**), with three carbon atoms bridging the two tetrahydroindenyl ligands. They observed that the axial symmetry of the ethylene-bridged congener, $Et(IndH_4)_2TiCl_2$ (**4**), was destroyed by a nonsymmetric location of the $(CH_2)_3$ bridge in complex **3**. The trimethylene bridge in **3** apparently requires a sufficiently longer distance between the bridgehead carbon atoms than that required for an ethylene bridge in **4**, resulting in an increase in the centroid–Ti–centroid angle of **3**. Dolle et al.[3] pointed out the influence of the length of the bridging group on the stereospecific α-olefin polymerization. Recently, Hollis and co-workers[17] characterized the structure of a titanium cyclacene complex, [(*S*,*S*)-Ti((*R*,*R*)-cyclacene)Cl_2] (**5**), which has the two tetrahydroindenyl ligands bridged with four carbon atoms of a *trans*-1,2-dimethylenecyclopentane group and shows C_1 symmetry in the solid state. They also proposed that the bridging group with more than two carbon atoms tends to expand the Cp tilt angle, leading to the C_1 structure which is not ideal for stereospecific polymerization. Furthermore, Herrmann et al.[4] repeated the synthesis and polymerization of the [$(Me_2SiCH_2CH_2SiMe_2)(Ind)_2$]$ZrCl_2$ (**6**) catalyst with two carbon and two silicon atoms as an *ansa* bridging group. Complex **6** is an ethylene-selective catalyst and is completely inactive toward propylene due to shielding of the reaction center of the catalyst by the bulky bridge and by the indenyl ligand directed toward the $ZrCl_2$ moiety. In this study, the properties of both ethylene and propylene polymerizations with the [$Zr\{C_6H_4(CH_2\text{-}1\text{-}C_9H_6)_2\text{-}1,2\}Cl_2$] (**1**) complex are investigated to determine the effect of a long, rigid chain of four carbon atoms as a bridging group in chiral metallocene catalysts on the activity and stereoselectivity in α-olefin polymerization. Polymerization data of catalyst **1**/MAO have been compared with those of the well-known C_2 symmetric, isospecific metallocene, *rac*-Et(Ind)$_2$-$ZrCl_2$ (**2**).

Experimental Section

Polymerization-grade ethylene (Daelim Ind. Co., Korea) and propylene (Korea Petrochem. Ind. Co., Korea) and extra-pure-grade nitrogen were further purified by passing through columns of Fisher RIDOX and 5A/13X molecular sieves. Extra-pure-grade toluene (J. T. Baker Inc., Phillipsburg, NJ) and analytical-grade tetrahydrofuran (THF; J. T. Baker Inc.) were further purified by refluxing over sodium metal in a nitrogen atmosphere. The other materials were purchased from Aldrich Chemical Co., Inc., and were used without further purification.

The *ansa*-ligand, bis(1-indenyl)-*o*-xylene, was prepared in 90% yield according to the reported synthetic method of bis(1-indenyl)ethane[5,13,14,18] by replacing 1,2-dibromoethane with α,α′-dibromo-*o*-xylene as a source of the bridging group. ^1H NMR (300 MHz, $CDCl_3$, 25 °C): δ 7.43–7.16 (multiplet, 12H), 5.91 (triplet, 2H), 3.87 (doublet, 4H), 3.23 (doublet, 4H). ^{13}C NMR (300 MHz, $CDCl_3$, 25 °C): δ 145.2, 144.5, 143.1, 137.7, 130.1, 130.0, 126.5, 126.0, 123.8, 37.6, 31.8. Mass spectrum: m/z 334 (M^+). Complex **1** was obtained from the reaction of dilithiated bis(1-indenyl)-*o*-xylene with $ZrCl_4$ in THF. The reaction of dilithiated bis(1-indenyl)-*o*-xylene with $ZrCl_4$ was also performed according to previously reported procedures[5,13,14,18] to produce a mixture of two diastereomers in a ratio of 1:1 (*rac*-**1**:*meso*-**1**) in 51% yield. Fractional recrystallization in dichloromethane–ether at −20 °C gives *rac*-**1** as

---

[*] To whom all correspondences should be addressed.

[†] Department of Chemical Engineering.

[‡] Department of Chemistry.

[®] Abstract published in *Advance ACS Abstracts,* May 15, 1995.

0024-9297/95/2228-4801$09.00/0

bright yellow crystals, and subsequent recrystallization in dichloromethane–hexane produces *meso*-**1** as a yellow solid. *rac*-**1**: ^{1}H NMR (300 MHz, $CDCl_3$, 25 °C) δ 7.61–7.10 (multiplet, 12H), 6.14 (doublet, 2H), 5.76 (doublet, 2H), 4.29 (doublet of doublet, 4H). Mass spectrum: m/z 492 (M^+). *meso*-**1**: ^{1}H NMR (300 MHz, $CDCl_3$, 25 °C) δ 7.65–7.09 (multiplet, 12H), 6.02 (doublet, 2H), 5.90 (doublet, 2H), 4.14 (doublet of doublet, 4H). Mass spectrum: m/z 492 (M^+).

Compound **2** was synthesized as previously described.[5,13,14,18] MAO was prepared from the direct hydrolysis of trimethylaluminum (TMA): TMA (300 mL, 2 M in toluene) was cooled to −60 °C in a 1000-mL flask equipped with a magnetic stirrer, nitrogen inlet, and syringe pump to control the addition rate of H_2O. Water (10.8 mL) was added dropwise over 2 h. Then, the mixture was warmed slowly to room temperature and stirred for 24 h. The product was separated by filtration, and MAO was recovered from the filtrate.

Solution polymerizations in toluene were carried out using a Teflon magnetic spinbar for agitation at a total pressure of 1.2 atm in a 500-mL glass reactor. Toluene (200 mL) was introduced into the reactor, the temperature was increased to polymerization temperature, and then toluene was saturated with monomer. A prescribed amount of MAO and a given metallocene dissolved in toluene were injected into the reactor by a tuberculin syringe, and then the polymerization was started. The polymerization rate was determined at 0.01-s intervals from the rate of monomer consumption and measured by a hot-wire flowmeter (Model 820 from Sierra Instrument) connected to a personal computer through an A/D converter. Polymerization productivities were estimated by comparing the consumption rate of monomer recorded in the computer with the polymer yield. Results agreed within ±5% with the actual yield of polymer after polymerization. All the runs were stopped by injecting ethanol to kill the active polymerization sites, and the polymers were precipitated by the addition of an excess of acidified methanol. The precipitated polymer was recovered by filtration, washed with fresh ethanol, and dried *in vacuo*.

^{13}C-NMR (75 MHz) spectra of the polymer were recorded at room temperature on a Bruker AMX-300 FT NMR spectrometer. The samples in a 10-mm-o.d. glass tube were dissolved in $CDCl_3$ at 50 °C. The melting points of polymers were determined from the peaks of the DSC curves obtained with a Du Pont Analyst 2000 differential scanning calorimeter at a heating rate of 20 °C/min. The intrinsic viscosity, $[\eta]$, of the polymer in decalin was determined using a modified Ubbelohde viscometer at 135 ± 0.1 °C by one-point intrinsic viscosity.[19] The viscosity-average molecular weight (M_v) of polypropylene was calculated from the following equation:[20]

$$[\eta] = 1.0 \times 10^{-4} M_v^{\,0.80}$$

Results and Discussion

The required ligand, bis(1-indenyl)-*o*-xylene, is obtained by reaction of α,α'-dibromo-*o*-xylene with 2 equiv of indenyllithium. Complex **1** is prepared from the reaction of dilithiated bis(1-indenyl)-*o*-xylene with $ZrCl_4$ in a diastereomeric ratio of 1:1 (*rac*-**1**:*meso*-**1**). The two diastereomers are separated by fractional recrystallization. The diastereomer assignment is based on the preparation of the dimethyl derivatives of complex **1**. The dimethyl derivatives were prepared from the reaction of dilithiated bis(1-indenyl)-*o*-xylene with $Zr(CH_3)_2Cl_2$ in THF. One dimethyl derivative with a single ^{1}H NMR methyl resonance at δ −1.24 reacts with HCl to give *rac*-**1**, whereas the other dimethyl derivative with two CH_3 resonances at δ −0.36 and −2.91 affords *meso*-**1**. Details of the synthesis and characterization of the dimethyl derivatives will be reported elsewhere.

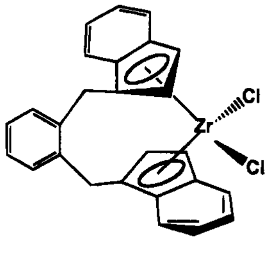

racemic-**1**

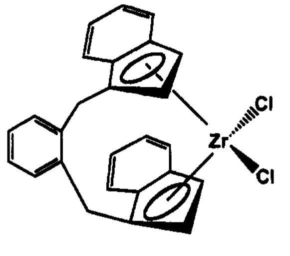

meso - **1**

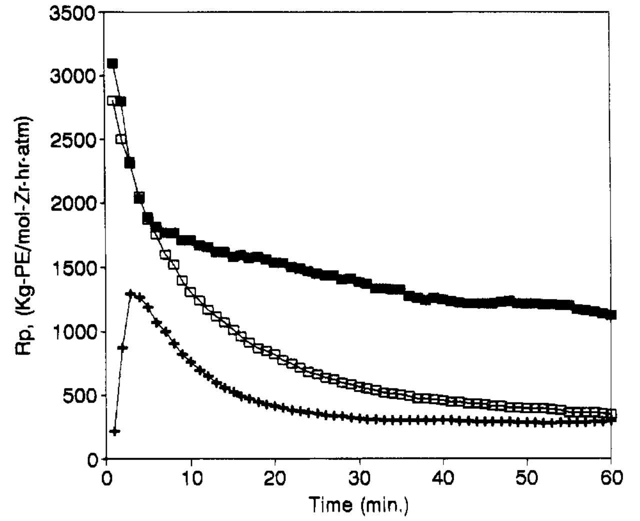

Figure 1. Ethylene polymerization rate profiles with *rac*-**1**/MAO catalyst at different temperatures: (+) 30, (□) 50, (■) 70 °C. Polymerization conditions: ethylene pressure, 1.2 atm; solvent, toluene, 200 mL; [Zr] = 2.0 × 10^{-5} M; [Al] in MAO, 0.2 M.

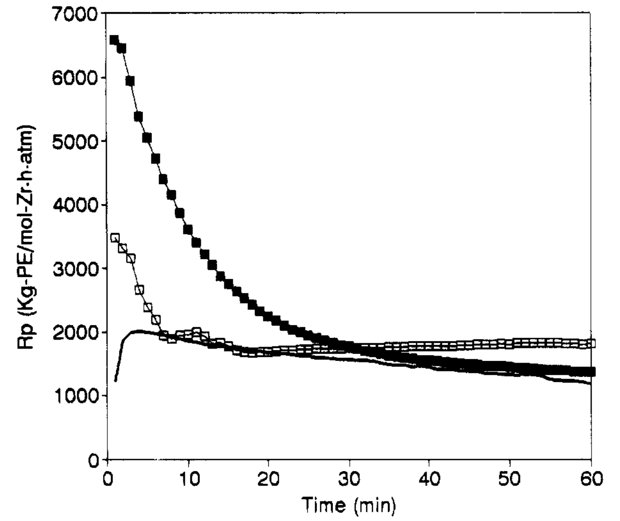

Figure 2. Ethylene polymerization rate profiles with *meso*-**1**/MAO catalyst at different temperatures: (—) 30, (□) 50, (■) 70 °C. Polymerization conditions: ethylene pressure, 1.2 atm; solvent, toluene, 200 mL; [Zr] = 2.0 × 10^{-5} M; [Al] in MAO, 0.2 M.

Figures 1 and 2 show the polymerization profiles for ethylene polymerization with *rac*-**1** and *meso*-**1** cocatalyzed with MAO ([Al]/[Zr] = 10 000) at three different temperatures, respectively. As shown in Table 1, the catalytic activity of the *rac*-isomer is lower and more influenced by the polymerization temperature than that of the *meso*-isomer. The results imply that, in ethylene polymerization with the **1**/MAO catalyst system, the coordination of ethylene to the active metal species is more difficult in *rac*-**1** than in *meso*-**1**. The polymerization rate profiles, however, are similar in both the *racemic* and *meso* isomers (see Figures 1 and 2). The

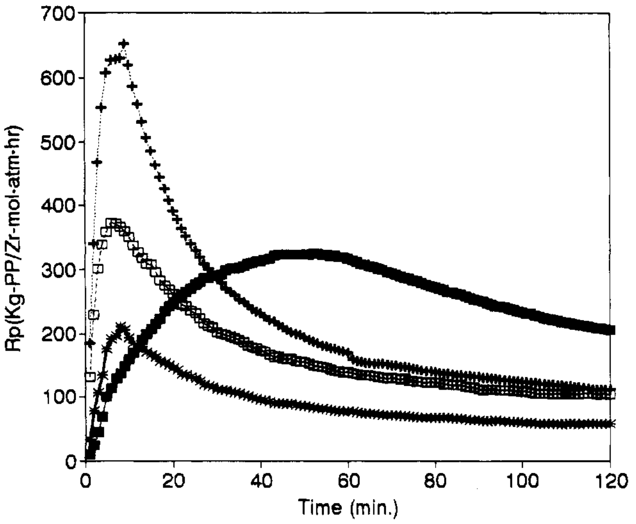

Figure 3. Propylene polymerization rate profiles with *rac*-**1**/MAO catalyst at different temperatures: (■) 0, (+) 30, (□) 50, (*) 80 °C. Polymerization conditions: propylene pressure, 1.2 atm; solvent, toluene, 200 mL; [Zr] = 2.0 × 10^{-5} M; [Al] in MAO, 0.2 M.

Table 1. Catalytic Activities of *rac*-1 and *meso*-1 Cocatalyzed with MAO in the Ethylene Polymerization

catalyst	T_p (°C)	average activity (kg-PE/mol-Zr·h·atm)
rac-1	70	1470
	50	830
	30	450
meso-1	70	2400
	50	1900
	30	1560

shapes of the polymerization profile at both 50 and 70 °C (the decay type kinetic curve) are similar to those of ethylene polymerizations with Cp_2ZrCl_2/MAO systems:[21,22] the polymerization rate reaches a maximum within a very short time and then gradually decreases. In contrast, the kinetic profile at 30 °C shows an induction period of 3–7 min. These results suggest that the active-site formation in the reaction of chiral metallocene complex **1** with MAO is slow at low temperatures.

In contrast to the ethylene polymerization, propylene polymerization occurs only with *rac*-**1**. The very low activity of propylene polymerization with *meso*-**1** is observed at a monomer pressure of 8.5 atm and in the temperature range of 0–80 °C. Only a very small amount of PP was produced for the initial 3–10 min of polymerization, and no activity was observed thereafter. Collins and co-workers[23] also reported that the activity of *meso*-$Et(IndH_4)_2ZrCl_2$ (**7**) is much less in propylene polymerizations than that of the *racemic* isomer. The *meso*-isomer, presumably, interacts with MAO most strongly on the less hindered side. If it is assumed that the growing polymer chain occupies the central site, incoming monomer will thus be forced to coordinate from the remaining lateral site that is sterically blocked by the six-membered ring of tetrahydroindene. The low activity of the *meso*-**1** in propylene polymerizations can be explained in an analogous manner to *meso*-**7**.

Figure 3 shows propylene polymerization rate profiles at 0, 30, 50, and 80 °C catalyzed by the *rac*-**1**/MAO catalyst. It takes about 50 min to reach the maximum rate at 0 °C, while only a short induction period (ca. 10 min) is observed in the polymerizations at higher temperatures (30–80 °C). The longer induction period relative to ethylene polymerization indicate that it takes longer to form the active centers for propylene polymerization than for ethylene polymerization. The average polymerization rate over a 120 min period decreased with an increase in the temperature in the propylene polymerization in contrast with the ethylene polymerization. This negative temperature effect in propylene polymerization seems to be related to the structure of *rac*-**1** with the twisted bridging ligand and its fluxionality at higher temperatures. Hollis and co-workers[17] reported that, in titanium complex [(*S*,*S*)-Ti((*R*,*R*)-cyclacene)Cl_2] (**5**), the tetrahydroindenyl ligands are twisted so that one ring projects at one of the chloro ligands while the other is twisted away from the other chloro ligand and the cyclacene bridge is unsymmetrically disposed with respect to the bisector of the Cl–Zr–Cl angle as shown by a single-crystal X-ray diffraction study. It, however, was observed that complex **5** in solution is symmetrical based on the ^{1}H-NMR spectrum because it undergoes a rapid conformational interconversion between two equivalent C_1 structures by rotation of the π-ligand via a C_2 symmetric structure in solution. The ^{1}H-NMR spectra of both *rac*-**1** and *meso*-**1** reveal that they are also symmetrical in solution. The conformational interconversion in *rac*-**1** seems to make the insertion of propylene monomer slower than that of the metallocenes with a stable C_2 symmetry. The low activities of propylene polymerization with *rac*-**1** at higher temperatures can also be explained by the rapid interconversion between the two C_1 structures, so that the insertion of propylene monomer is sterically more hindered at higher temperatures.

Table 2. Properties of PP Polymerized with a *rac*-1/MAO Catalyst System

		results of Soxhlet extraction (%)				
run[a] no.	T_p (°C)	hexane soluble	hexane insoluble, heptane soluble	heptane insoluble	intrinsic viscosity	$\overline{M}_v$
1	−20	85.1	3.5	11.4	*b*	
2	0	87.9	5.6	6.6	1.92	226 000
3	25	85.4	10.5	4.1	2.42	301 000
4	30	82.5	14.9	2.6	2.46	308 000

[a] Polymerization conditions: [Zr] = 2.0 × 10^{-5} M; [Al] in MAO, 0.2 M; solvent, toluene, 200 mL; propylene pressure, 1.2 atm (run nos. 1 and 2) and 8.7 atm (run nos. 3 and 4). [b] No measurement.

Table 2 shows the physical properties of PP's prepared with the *rac*-**1**/MAO catalyst at four different temperatures. As shown in the solvent fractionation, over an 85% fraction of all the polymer samples is soluble in boiling hexane. The boiling heptane-insoluble fractions of all the PP's were also very low (below 12%), although the insoluble fraction of PP obtained at low polymerization temperature was slightly larger than that obtained at higher temperatures. The melting points of all the polymer samples could not be detected. These results indicate that the *rac*-**1**/MAO catalyst with the *ansa*-ligand distorted by a four-carbon bridge does not produce stereoregular polymers.

As shown in Table 3, the ethylene polymerization activity of the *rac*-**1**/MAO catalyst at 50 °C is about 20% of that of **2**/MAO, and T_m of PE produced by *rac*-**1**/MAO is higher than that of PE produced by **2**/MAO. In the case of propylene polymerization, *rac*-**1**/MAO is much less active than **2**/MAO at 30 and 50 °C. On the contrary, the polymerization activity of *rac*-**1**/MAO at 0 °C is higher than that of **2**/MAO. This suggests that *rac*-**1**/MAO has a lower activation energy for propylene polymerization than that of **2**/MAO and may form active

Table 3. Comparison of the *rac*-1/MAO Catalyst System with 2/MAO in the Ethylene and Propylene Polymerization

monomer	catalyst	T_p (°C)	time (h)	activity[a]	T_m (°C)	heptane-insoluble (%)
ethylene	**2**/MAO	50	3	4300	133.8	
	rac-**1**/MAO	30	1	452	142.0	
		50	1	831	134.7	
		70	1	1470	129.0	
propylene	**2**/MAO	50	3	3000	125.1	17.5
		30	3	1500	133.0	57.5
		0	3	110	147.5	74.6
	rac-**1**/MAO	50	2	170		0
		30	2	230		2.6
		0	2	265		6.6

[a] Units are kg-polymer/mol-Zr·h·atm.

Table 4. Steric Sequence Distributions of PP Obtained with the *rac*-1/MAO Catalyst System at 0 and 30 °C

		T_p (°C)	
		0	30
pentad	mmmm	0.357	0.284
	mmmr	0.138	0.109
	rmmr	0.060	0.051
	mmrr	0.170	0.155
	mrmm + rmrr	0.110	0.127
	rmrm	0.062	0.104
	rrr	0	0.032
	rrrm	0.067	0.057
	mrrm	0.046	0.081
triad	mm	0.552	0.445
	mr	0.317	0.393
	rr	0.131	0.172
diad	m	0.711	0.642
	r	0.289	0.358
triad tests[a]	2[rr]/[mr]	0.83	0.87
	$4[rr][mm]/[mr]^2$	2.88	1.96

[a] $2[rr]/[mr] = 2S/H = 1$ for an enantiomorphic site control model and $4[rr][mm]/[mr]^2 = 4SI/H^2 = 1$ for a chain end control model.

polymerization centers more easily at 0 °C than **2**/MAO. The melting points of PE obtained with the *rac*-**1**/MAO catalyst decreased with an increase of the polymerization temperatures. The melting temperature of PE prepared with *rac*-**1** at 30 °C is 142.0 °C. The usual melting points are in the range of 132−135 °C in the case of HDPE (high-density polyethylene) prepared with a Ziegler−Natta catalyst.[24] If PE is completely crystallized due to complete packing of the chain, the melting point will be 141.1 °C.[25] The PE obtained with *rac*-**1**/MAO seems to be the HDPE of a very high crystalline structure.

Figure 4 shows the ^{13}C-NMR spectra of the methyl pentad of PP obtained with the *rac*-**1**/MAO system at 0 and 30 °C. Table 4 shows the integrated values of the chemical shifts of the methyl pentad stereosequences. The fraction of an isotactic pentad sequence (mmmm) of PP, 0.36, obtained at 0 °C is greater than that of PP, 0.28, obtained at 30 °C.

Figure 5 shows the ^{13}C-NMR spectrum of PP polymerized over *meso*-**1**/MAO at 30 °C. The *meso* pentad sequence of PP with *meso*-**1** is also a little lower than that with *rac*-**1**.

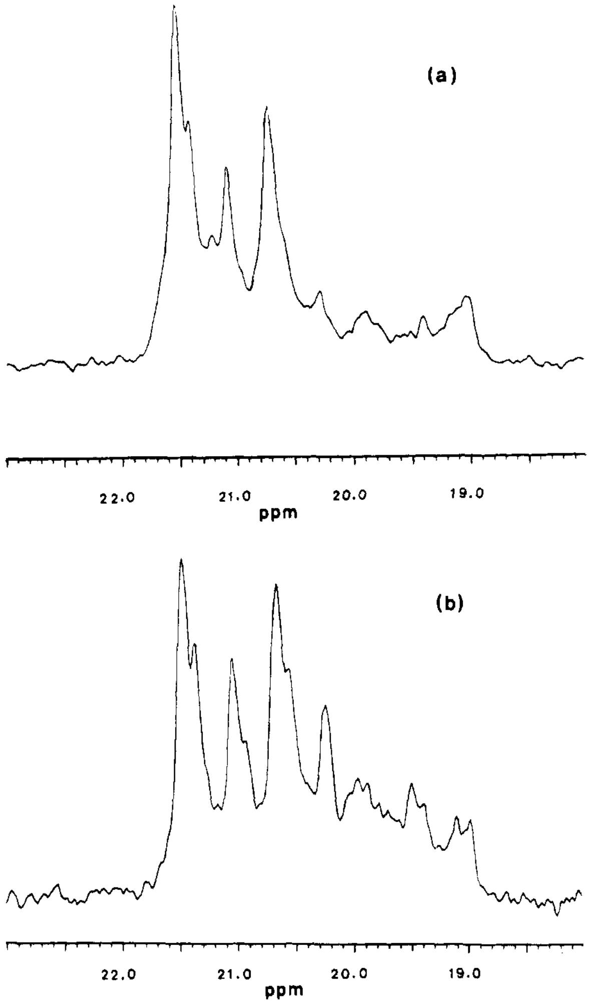

Figure 4. ^{13}C NMR spectra (methyl signal region) of polypropylene polymerized with a *rac*-**1**/MAO catalyst: (a) at 0 °C and (b) at 30 °C.

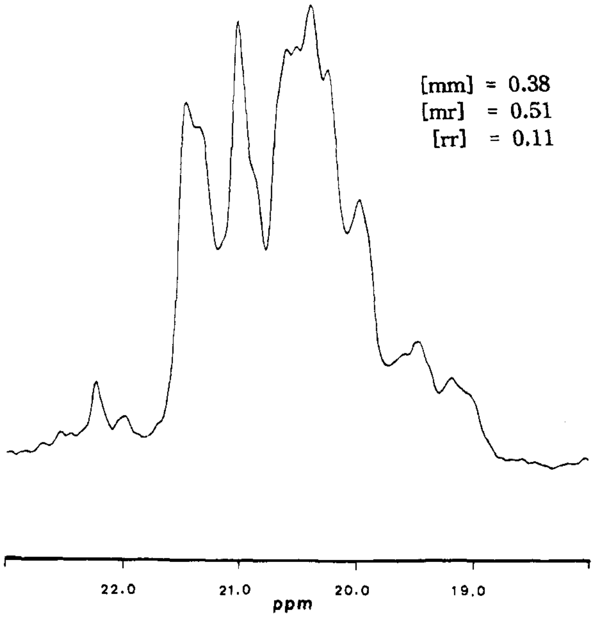

Figure 5. ^{13}C NMR spectrum (methyl signal region) of PP prepared with a *meso*-**1**/MAO catalyst (T_p, 30 °C; propylene pressure, 8.5 atm; solvent, toluene, 500 mL).

The stereochemical mechanism can be inferred from the tests of triad sequences.[26] If the value of $4[mm][rr]/[mr]^2$ is equal to 1, the distributions of the polymers are in accord with the Bernoullian statistical model, leading to stereochemical control by the configuration of the last inserted monomer unit. In contrast, if the value of 2[rr]/[mr] is equal to 1, the configurational microstructure of the polymer represents the isoblock which is consistent with the enantiomorphic site propagation model based on stereochemical control by the chirality of the catalyst. As shown in Table 4, the tests of triad methyl sequences are not consistent either with the chain end control mechanism or with the enantiomorphic site control mechanism. The microstructure of the PP sample obtained with *rac*-**1**/MAO also seems to be related to the fluxionality of catalyst **1** (*vide supra*), which causes the orientation of the propylene monomer during insertion to be irregular.

Conclusions

The *meso*-**1**/MAO catalyst is more active than the *rac*-**1**/MAO in the ethylene polymerization. In propylene polymerization, however, the *rac*-**1**/MAO catalyst is active and the *meso*-**1**/MAO is almost inactive. Ethylene polymerization activity with *rac*-**1**/MAO increases as the temperature increases. The inverse temperature effect is observed for propylene polymerization with the *rac*-**1**/MAO catalyst system. Based on the results of solvent fractionation and ^{13}C NMR spectroscopy, stereoregularity of PP is much lower than that of the well-known C_2 symmetric *rac*-**2** catalyst. Our results suggest that, for *rac*-**1** bridged with four carbon atoms, the two π-ligands are distorted by the long chain bridge, leading to a C_1 structure to give low stereoregularity in propylene polymerization. Furthermore, rate profiles at different temperatures indicate that the *rac*-**1** catalyst undergoes a rapid, rotational interconversion of the indenyl ligands via a C_2 symmetric structure, which interrupts the insertion of propylene monomer resulting in a decreased polymerization rate at higher temperatures.

Acknowledgment. This research was funded by the National Project granted from the Ministry of Science and Technology (NN09260) and by the Catalysis Technology Research Center at POSTECH (1991–1994). Ethylene gas was kindly donated by Daelim Ind. Corp. and propylene by Korea Petrochem. Corp.

References and Notes

(1) Bierwagen, E. P.; Bercaw, T. E.; Goddard, W. A. *J. Am. Chem. Soc.* **1994**, *116*, 1481.

(2) Spaleck, W.; Winter, F. K.; Rohrmann, J.; Bachmann, B.; Antberg, M.; Dolle, V.; Paulus, E. F. *Organometallics* **1994**, *13*, 954.

(3) Antberg, M.; Dolle, V.; Klein, R.; Rohrmann, J.; Spaleck, W.; Winter, A. In *Catalytic Olefin Polymerization*; Keii, T., Soga, K., Eds.; Elsevier: New York, 1990; pp 501–515.

(4) Herrmann, W. A.; Rohrmann, J.; Herdtwerck, E.; Spaleck, W.; Winter, A. *Angew. Chem., Int. Ed. Engl.* **1989**, *28*, 1511.

(5) Lee, I. M.; Gauthler, W. J.; Ball, J. M.; Iyengar, B.; Collins, S. *Organometallics* **1992**, *11*, 2115.

(6) Erker, G.; Nolte, R.; Aul, R.; Wilker, S.; Kruger, C.; Noe, R. *J. Am. Chem. Soc.* **1991**, *113*, 7594.

(7) Chien, J. C. W.; Song, W.; Rausch, M. D. *Macromolecules* **1993**, *26*, 3239.

(8) Resconi, L.; Abis, L.; Franciscono, G. *Macromolecules* **1992**, *25*, 6814.

(9) Ewen, J. A.; Haspeslagb, L.; Atwood, J. L.; Zhang, H. *J. Am. Chem. Soc.* **1987**, *109*, 6544.

(10) Ewen, J. A.; Robert, L. J.; Razavi, A.; Ferrara, J. D. *J. Am. Chem. Soc.* **1988**, *110*, 6255.

(11) Spaleck, W.; Antberg, M.; Rohrmann, J.; Winter, A.; Bachmann, B.; Kiprof, P.; Behm, J.; Herrmann, A. *Angew. Chem., Int. Ed. Engl.* **1992**, *31*, 1347.

(12) Wiesenfelt, H.; Reinmuth, A.; Barties, H.; Evertz, K.; Brintzinger, H. H. *J. Organomet. Chem.* **1989**, *369*, 359.

(13) Wild, F. R. W. P.; Wasiucionek, M.; Huttner, G.; Brintzinger, H. H. *J. Organomet. Chem.* **1985**, *288*, 63.

(14) Wild, F. R. W. P.; Zsolnai, L.; Huttner, G.; Brintzinger, H. H. *J. Organomet. Chem.* **1982**, *232*, 233.

(15) Gutmann, S.; Burger, P.; Hunt, H. U.; Hofmann, J.; Brintzinger, H. H. *J. Organomet. Chem.* **1989**, *369*, 343.

(16) Roll, W.; Zsolnai, L.; Huttner, G.; Brintzinger, H. H. *J. Organomet. Chem.* **1987**, *322*, 65.

(17) Hollis, T. K.; Rheingold, A. L.; Robinson, N. P.; Whelan, J.; Bosnich, B. *Organometallics* **1992**, *11*, 2812.

(18) Collins, S.; Kuntz, B. A.; Taylor, N. J.; Ward, D. G. *J. Organomet. Chem.* **1988**, *342*, 21.

(19) Elliott, J. H. *J. Appl. Polym. Sci.* **1970**, *19*, 2947.

(20) Chiang, R. *J. Polym. Sci.* **1958**, *35*, 235.

(21) Chien, J. C. W.; Wang, B. P. *J. Polym. Sci., Part A: Polym. Chem.* **1988**, *26*, 3089.

(22) Chien, J. C. W.; Wang, B. P. *J. Polym. Sci., Part A: Polym. Chem.* **1989**, *27*, 1539.

(23) Collins, S.; Gauthier, W. J.; Holden, D. A.; Kuntz, B. A. Taylor, N. J.; Ward, D. Z. *Organometallics* **1991**, *10*, 2061.

(24) Arakawa, T.; Wanderich, B. *J. Polym. Sci., Polym. Phys. Ed.* **1966**, 53.

(25) Richardson, M. T.; Florry, P. J.; Jacson, J. B. *Polymer* **1963**, *4*, 221.

(26) Ewen, J. A. *J. Am. Chem. Soc.* **1984**, *106*, 9355.

MA946259H